Journal of
Archaeological
SCIENCE

Avian resource depression or intertaxonomic variation in bone density? A test with San Francisco Bay avifaunas

Jack M. Broughton*, Daniel Mullins, Tamara Ekker

Department of Anthropology, University of Utah, Salt Lake City, UT 84112-0060, United States

Abstract

Previous analyses of the Emeryville Shellmound fauna suggested that ever-expanding late Holocene human populations of the San Francisco Bay area depressed a wide range of vertebrate taxa, including cormorants (*Phalacrocorax*), geese (Anserinae), and large shorebirds (e.g., *Numenius*, *Limosa*). Far-reaching implications for prehistoric human behavior, historical ecology, and modern conservation biology have resulted from that work. We test the generality of the bird-based conclusions here by documenting temporal trends in avifaunal abundances from five additional sites located on the San Francisco Peninsula. Analyses of these data reveal patterns identical to those found at Emeryville, showing significant declines through time in the relative abundances of both geese and cormorants between about 2000 and 700 B.P. New photon absorptiometric-based density data for cormorants, geese, and ducks (Anatinae) are used to determine if the declines through time in the relative abundances of geese and cormorants are correlated with variation in the extent of density-mediated attrition observed in these faunas. The data and analyses presented here suggest that while density-mediated attrition played a role in structuring element abundances in these avifaunas, there is no evidence that it varied systematically through time to produce the revealed patterns in taxonomic abundances. Resource depression thus remains a viable hypothesis for the declining abundances of large-sized waterbirds during the late Holocene of the San Francisco Bay region. The new bone density data we present should be useful to analyses of archaeological and paleontological avifaunas wherever these or related taxa are found around the world.
© 2006 Elsevier Ltd. All rights reserved.

Keywords: Density-mediated attrition; Taphonomy; Resource depression; San Francisco Bay; Avifaunas; Zooarchaeology; Human impacts

1. Introduction

Over the last decade, there has been a great surge of interest in prehistoric *resource depression*, or declines in the capture rates of prey that result from the activities of foragers. These studies reflect a growing interest in understanding the role that native peoples played in structuring and impacting the environments in which they lived. Faunal resource depression and the resulting declines in foraging efficiency also carry implications for numerous aspects of prehistoric human health and may be linked to many important behavioral transitions in human prehistory. Perhaps most significantly, the documentation of resource depression also entails implications for historical ecology and modern conservation biology.

In the late Holocene of California, for instance, resource stress resulting from the depression of a wide range of vertebrate prey types has been causally linked to increases in human violence, warfare, and territoriality, reduced stature, declining health, technological changes, and the emergence of hereditary inequalities. A long-held *utopian* perception of aboriginal lifeways—a cornerstone of California ethnography and archaeology—is undercut by this work as well [12,16,39]. The evidence for prehistoric resource depression is also

* Corresponding author.
E-mail address: jack.broughton@anthro.utah.edu (J.M. Broughton).

directly relevant to the modern management of regional wilderness and wildlife because it reveals past conditions and processes that can inform on the creation of ecological benchmarks [13,14,30,51].

Prehistoric resource depression is now routinely measured with taxonomic abundance data using foraging theory logic, independently derived in zoology [63] and archaeology [2,3]. From the prey model [59], it is predicted that the most energetically profitable or highest-return prey will be taken whenever they are encountered—the selection of lower-return prey, however, depends on the abundance of the former. It follows that the relative frequency with which foragers selected high- and low-ranked prey can provide indices of both the encounter rates of the high-ranking ones and within-patch foraging efficiency. *Declining* relative abundances of high-return prey can then signal resource depression if other causes, such as environmental change, can be ruled out [2,8,9,11,13,15].

Other evidence, such as prey age structure to reveal harvest pressure or skeletal part representation to detect local depletion and distant patch use, have also been deployed to corroborate the evidence for depression suggested by taxonomic abundance data [11,13,14,60,62]. Prehistoric resource depression using this methodology has now been documented in a wide range of temporal-geographic contexts around the globe and has involved a wide range of taxa—from tortoises (*Testudo*) in the Middle Paleolithic of Italy, to bighorn sheep (*Ovis canadensis*) in the Great Basin during the late Holocene [29,30,60; see also 17,20,36—38,50,53,57].

Yet despite this now extensive body of literature, there are only a few cases outside of insular oceanic contexts that have provided detailed evidence for anthropogenic depressions of prehistoric bird populations [5,14]. One of those was recently documented from analyses of the rich avifauna from the Emeryville Shellmound, a large, stratified site once located on the eastern shore of San Francisco Bay (Fig. 1). In this context, ever-expanding late Holocene populations appear to have depressed a wide range vertebrate taxa, including birds such cormorants (*Phalacrocorax*), geese (Anserinae), and large shorebirds (e.g., *Numenius, Limosa*) [11,13,14].

In previous analyses of resource depression, there has also been virtually no attention devoted to evaluating intertaxonomic differences in bone density as a potential factor influencing temporal declines in the abundances of large-sized, high-return vertebrate prey. There are, however, obvious reasons for thinking that bone density could play an important role in influencing trends in taxonomic abundances. If the bones from larger, higher-return taxa, for example, have higher densities than smaller species, and both density and exposure time in sediments determines survivorship, we could expect older sediments to contain higher proportions of large-sized taxa. Temporal declines in the abundances of larger vertebrate taxa may be telling us very little about resource depression and everything about density-mediated attrition.

We address this general issue here by conducting an independent test of the hypothesis that prehistoric foragers of the San Francisco Bay depressed the regions waterfowl (Anatidae) and cormorant populations. We first present temporal trends in avifaunal abundances from five additional sites in the San Francisco Bay area. We then present the first photon absorptiometric-based bone density data for cormorants, geese and ducks (Anatinae), the best-represented groups of birds in San Francisco Bay shellmounds. These data are then used to evaluate the degree to which the documented temporal trends in avian abundance indices may have resulted from density-mediated attrition. Although we present these new density data in the context of testing a specific hypothesis here, they should be useful to the analyses of archaeological and paleontological avifaunas wherever these or related taxa are found around the world.

2. Measures of avian resource depression and trends from the Emeryville sequence

As noted above, recent analyses of the Emeryville Shellmound avifauna suggested that prehistoric hunters had significant impacts on the bird populations of the San Francisco Bay area. Those analyses were based on 5736 identified avian specimens derived from stratified sediments deposited between 2600 and 700 ^{14}C yr B.P. [14]. Since we provide independent tests of that conclusion here, we first summarize key aspects of the methodology used and trends observed in the Emeryville study.

In the Emeryville analysis, Broughton [14] derived several taxonomic abundance measures to detect avian resource depression. Following earlier work with mammals and fishes, prey body size was used as a proxy measure of prey rank for bird taxa that arguably would not have exhibited significant differences in handling costs (see [61] for a systematic evaluation of the relationship between prey size and return rate). Accordingly, Broughton [14] reasoned that avian resource depression should be signaled by declining relative abundances of large-sized taxa, other things being equal (see [13,14] for detailed discussion on the issues of prey spatial structure, habitat affinities, and hunt types in relation to taxonomic indices of prey depression).

Significant declines through time in the abundances of a variety of large-sized avian taxa were then documented from the Emeryville deposits using Cochran's test of linear trends, a chi-square based method that weights assemblages by their associated specimen sample sizes [21,64]. In the waterfowl assemblage, the larger-sized taxa—geese (e.g., *Branta canadensis, Anser albifrons, Chen caerulescens, Chen rossii*)—declined through time relative to ducks $\left(X^2_{\text{trend}} = 620.61, \text{ df} = 1, P < 0.001\right)$. Even the remains of the largest-sized geese taxa (e.g., *Branta canadensis moffitti, Anser albifrons, Chen caerulescens*) declined compared to the smaller ones (e.g., *Branta hutchinsii minima, Chen rossii*) $\left(X^2_{\text{trend}} = 12.32, \text{ df} = 1, P < 0.001\right)$.

Within the shorebird collection, the largest species—Marbled Godwits (*Limosa fedoa*), Long-billed Curlews (*Numenius americanus*), and Whimbrels (*Numenius phaeopus*)—declined through time, relative to smaller shorebird taxa $\left(X^2_{\text{trend}} = 17.34, \text{ df} = 1, P < 0.001\right)$. Similarly, Double-crested cormorant (*Phalacrocorax auritus*) specimens are very
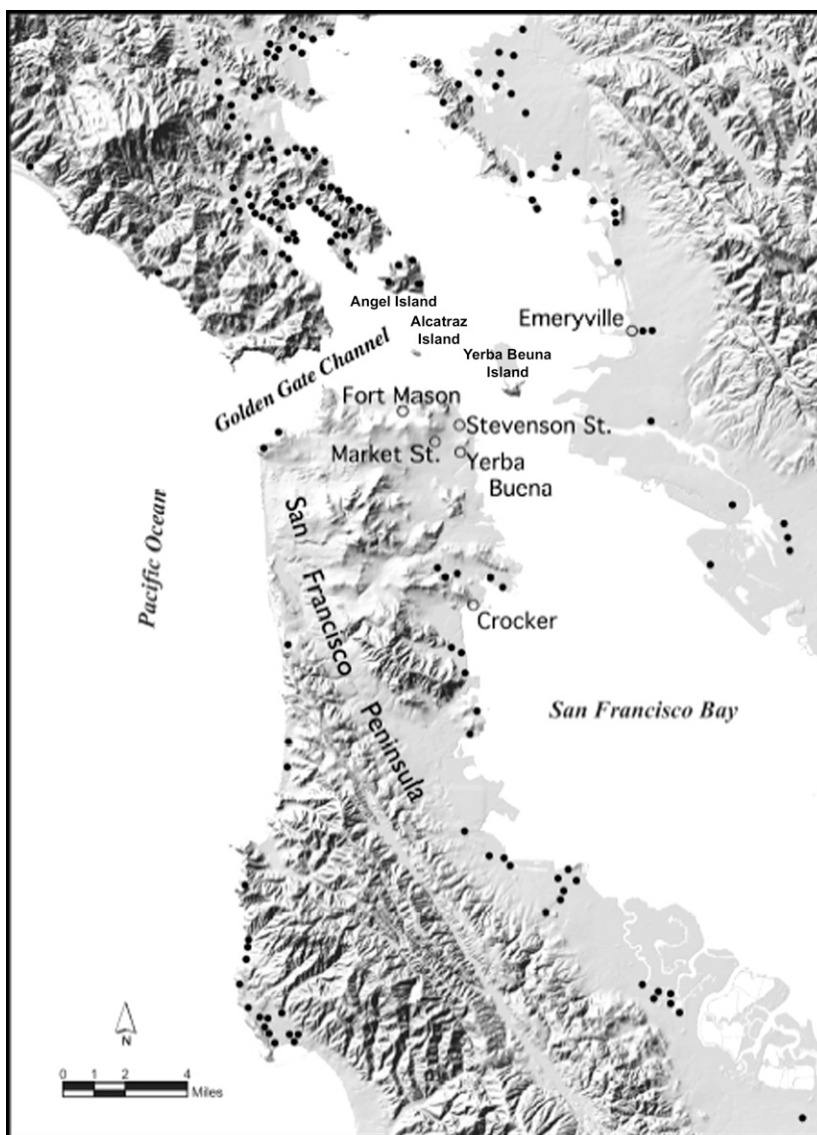
Fig. 1. Map of the San Francisco Bay area, showing the location of sites and other features discussed in the text, and other shellmounds recorded by Nelson [54].

abundant early-on in the site's history—including abundant material representing chicks and juveniles—but their numbers crash precipitously between about 1600 and 1300 ^{14}C yr B.P. $\left(X^2_{\text{trend}} = 585.55, \text{ df} = 1, P < 0.001; [14]\right)$.

Other patterns appear to reflect declining hunting returns from local patches and the ever-increasing use of more distantly located ones. For instance, marine-oriented duck taxa, namely scoters (*Melanitta fusca* and *M. perspicillata*), steadily increase in abundance through time compared to ducks that are associated with freshwater contexts and marshes found along the margins of the bay—closer to Emeryville $\left(X^2_{\text{trend}} = 54.54, \text{ df} = 1, P < 0.001; [14]\right)$.

None of these patterns were found to correlate with changes in pertinent paleoenvironmental records that might indicate they were caused by climate-based environmental change— not surprising, given that the trends were registered in bird taxa with widely disparate habitat affinities,

ecologies, and seasonal abundance patterns. The geese involved, for instance, are primarily winter visitants to marshes and terrestrial grasslands of the San Francisco Bay area and migrate to northern latitudes or the interior of the continent to breed during the spring and summer months. The larger shorebirds, on the other hand, reach their highest densities in local mudflat habitats during spring and fall migrations. And the piscivorous Double-crested cormorant is a resident colonial breeder on islands within the San Francisco Bay estuary [14].

To evaluate to what degree these trends reflect region-wide avian population declines we turn to a new set of avifaunal materials derived from five sites located about 10 km west of Emeryville on the San Francisco Peninsula (Fig. 1). Aside from Emeryville, more detailed avifaunal analysis has occurred for sites in this region than any other in the San Francisco Bay area [7,26,32,45,52].

3. Resource depression and the San Francisco Peninsula avifaunas

The San Francisco Peninsula is a 50-km long land mass bounded to the west by the Pacific Ocean, to the east by the brackish San Francisco Bay estuary and to the north by the Golden Gate Channel—the city of San Francisco now rests on its northern tip (Fig. 1). Prior to Gold Rush era development and urbanization, the San Francisco Peninsula was characterized by shifting sand dunes and a mosaic of terrestrial vegetation types including seaside, prairie scrub, and oak woodland communities. Extensive mudflats and tidal marshes also bordered the Peninsula's eastern margin [40,42].

Avifaunal identifications from previous studies are available from five sites in the region: the Crocker Mound (CA-SFR-07), the Fort Mason Shellmound (CA-SFR-29, 30, 31), the Yerba Buena Shellmound (CA-SFR-114), the Stevenson Street Shellmound (CA-SFR-112), and the Market Street Shellmound (CA-SFR-113). All but one of these sites were excavated between 1978 and 1988 in cultural resource management contexts associated with development in downtown San Francisco (Table 1). The exception is the Crocker Mound, a site excavated and briefly described by Nels Nelson in 1910 [58]. The faunal materials from these sites were collected with 1/4- and 1/8-inch screens, again with exception to the Crocker Mound; documentary photographs show Nelson's crew excavating the site with shovels but no screens [58]. We discuss the potential impact of the different recovery method used for this site below. All of the sites were located within a few kilometers of the San Francisco Bay and three of them were located within 2 km of each other (Fig. 1). The human occupational histories of these sites span the period from roughly 2000 to 700 ^{14}C yr B.P. (Table 1) and thus they fall within the time range that people lived across the bay at Emeryville (see [46] for details on the origins, history and diverse functions of San Francisco Bay area shellmounds).

We follow two approaches to test the hypothesis that prehistoric hunters depressed the regions avifauna with the San Francisco Peninsula collections. In the first, more coarse-grained approach, we examine relative abundance data from the collections at the site level. This strategy was required by the fact that most of the avian identifications for the San Francisco Peninsula assemblages were reported at the site level, rather than by stratigraphic subdivisions within them. Temporal trends are examined by comparing the abundances of different bird taxa for the sites as single units arrayed through time by the midpoints of their occupation ranges (Table 1, column 4). Chronological assignments were based on radiocarbon dating, time-sensitive artifact styles (especially shell beads), and obsidian hydration [1,9,34,55, 56,58].

In the second, intrasite approach, we focus on materials deposited across the occupational history of the Yerba Buena Shellmound—a site that produced by far the largest collection of avifaunal materials in the study sample and for which we provide identifications here by chronologically meaningful provenience units. In both approaches, we focus on the potential evidence for the depression of geese and cormorants—the collective shorebird sample size for these sites is very small (NISP = 67) and the vast majority (85%) of those specimens come from a single site (Table 2).

3.1. Intersite analysis

Table 2 provides the number of identified bird specimens (NISP) recovered from the five San Francisco Peninsula sites. The relative abundance of geese, compared to ducks, in these sites is arrayed through time in Fig. 2. Although a tight temporal trend is not apparent, geese do appear to dominate the waterfowl assemblages in the earlier sites, while ducks, in most cases, are more abundant in later deposits. A Cochran's test of linear trends confirms this impression, showing that a highly significant linear decline through time in the abundance of geese is present $\left(X^2_{\text{trend}} = 26.11, \text{df} = 1, P < 0.001\right)$.

The abundance of cormorants compared with that of all other birds from these sites is displayed in Fig. 3. Cormorants are most abundant in the oldest site in the sample—the Market Street Shellmound; this site was occupied between 2110 and 1830 B.P. and cormorants comprise nearly 40% of the identified avian sample. By contrast, cormorants comprise less than 4% of the bird materials in several of the sites occupied after 1500 B.P. A Cochran's test comparing the relative abundances of cormorant bones compared to those of all other birds in the five-site sample shows that this decline is highly significant $\left(X^2_{\text{trend}} = 149.15, \text{df} = 1, P < 0.001\right)$.

These trends do not appear to have been affected by the lack of screening at the Crocker Mound and the possible over-representation of larger taxa in that assemblage. In fact, the Crocker Mound represents the youngest site in the study sample and it provided among the lowest relative frequencies of geese and cormorants.

Table 1
Occupation dates and references for San Francisco Peninsula archaeological sites used in this analysis

Site	Occupation Date (B.P.)			Reference	
	Initial	Terminal	Median	Avifauna	Date
Crocker Mound (CA-SFR-7)	1650	650	1150	[52]	[58]
Fort Mason Shellmond (CA-SFR-29, 30, 31)	1450	1250	1350	[26]	[1]
Yerba Buena Shellmound (CA-SFR-114)	1950	1010	1480	[7]	[34]
Stevenson Street Shellmound (CA-SFR-112)	1790	1240	1515	[45]	[55]
Market Street Shellmound (CA-SFR-113)	2110	1830	1970	[32]	[56]

Table 2
Numbers of identified avian specimens per taxon for selected San Francisco Peninsula archaeological sites

Taxon	Crocker Mound	Fort Mason	Yerba Buena	Stevenson Street	Market Street	$\sum$
Gavia sp.	1	1	–	2	3	7
Gavia immer	–	1	–	–	–	1
Gavia stellata	–	–	1	–	–	1
Podicipedidae (small)	–	–	2	–	–	2
Podilymbus podiceps	–	–	1	–	–	1
Podiceps sp.	–	–	7	3	3	13
Podiceps nigricollis	–	2	1	–	–	3
Podiceps grisegena or *Aechmophorus occidentalis*	–	–	1	–	–	1
Aechmophorus occidentalis/clarki	–	1	1	3	1	6
Phoebastria sp.	–	–	–	3	–	3
Procellaridae cf. *Puffinus* sp.	–	–	1	–	–	1
Fulmarus glacialis	–	–	–	3	–	3
Hydrobatidae	–	–	–	3	–	3
Pelecanus sp.	1	4	–	–	–	5
Pelecanus occidentalis	–	2	1	–	1	4
Phalacrocorax sp.	4	22	12	11	–	49
Phalacrocorax auritus	–	4	8	–	84	96
Phalacrocorax pelagicus	–	3	–	–	–	3
Phalacrocorax penicillatus	–	5	–	–	–	5
Ardea herodias	–	–	3	–	–	3
Nycticorax nycticorax	–	–	1	–	–	1
Cathartes aura	–	–	–	–	1	1
Gymnogyps californianus	–	–	–	1	–	1
Anatidae	–	3	84	–	–	87
Anserinae	–	7	5	–	76	88
Branta sp.	–	2	–	–	–	2
Branta bernicla	13	–	–	–	–	13
Chen rossii/Branta bernicla/ B. huthchinsii cf. *minima*	15	1	839	12	–	867
Anser albifrons/Chen caerulescens/ Branta canadensis (med.)	14	5	109	3	–	131
Branta canadensis (large)	–		2	3	–	5
Anatinae	–	3	22	–	26	51
Anatinae (small)	–	–	97	–	–	97
Anatinae (med.)	–	–	62	–	–	62
Anatinae (large)	–	–	96	–	–	96
Anas sp.	–	4	–	4	–	8
Anas sp. (teals)	–	–	28	–	10	38
Anas sp. (medium)	1	2	1	3	–	7
Anas sp. (large)	–	–	5	–	–	5
Aythya sp.	21	2	–	4	–	27
Aythya/Melanitta sp.	–	–	2	–	–	2
Melanitta sp.	51	5	1	8	–	65
Melanitta perspicillata	–	3	–	–	–	3
Bucephala sp.	–	–	1	–	–	1
Lophodytes cucullatus	–	–	2	–	–	2
Mergus merganser	–	–	1	–	–	1
Oxyura jamaicensis	–	–	4	–	–	4
Accipitridae	–	–	5	–	–	5
Accipiter striatus	–	1	–	–	–	1
Accipiter cooperi	–	–	–	2	–	2
Haliaeetus leucocephalus	–	–	1	–	–	1
Buteo sp.	–	–	5	–	–	5
Buteo lineatus	–	–	–	5	–	5
Buteo jamaicensis	–	1	2	–	–	3
Falco mexicanus	–	–	1	–	–	1
Callipepla californica	1	–	4	–	1	6
Rallus longirostris	–	–	1	–	–	1
Fulica americana	–	3	4	–	–	7
Grus canadensis	–	–	1	–	–	1
Charadriiformes	–	–	3	–	–	3
Pluvialis squatarola	–	–	7	–	–	7

Table 2 (*continued*)

Taxon	Crocker Mound	Fort Mason	Yerba Buena	Stevenson Street	Market Street	$\sum$
Recurvirostra americana	–	–	2	–	–	2
Catoptrophorus semipalmatus	–	–	–	–	1	1
Scolopacidae	–	–	–	–	2	2
Scolopacidae (large)	–	–	24	–	4	28
Numenius phaeopus	–	–	1	–	–	1
Numenius americanus	–	–	17	–	–	17
Limosa fedoa	–	–	5	–	–	5
Calidris sp.	–	1	–	–	–	1
Limnodromus sp.	–	–	1	–	1	2
Phalaropus fulicaria	–	1	–	–	–	1
Sterna forsteri	–	–	–	2	–	2
Larus sp. (size indet.)	–	1	7	–	1	9
Larus sp. (small)	–	–	3	–	–	3
Larus sp. (large)	–	3	20	2	–	25
Uria sp.	–	24	4	3	–	31
Patagioenas fasciata	–	–	1	–	–	1
Strigiformes	–	–	1	–	–	1
Tyto alba	–	–	8	–	–	8
Bubo virginianus	–	2	–	–	–	2
Asio sp.	–	–	7	–	–	7
Aegolius acadicus	–	–	1	–	–	1
Passeriformes	–	–	3	–	1	4
Amphelocoma coerulescens	–	–	2	–	–	2
Corvus brachyrhynchos	–	2	9	7	2	20
Corvus corax	–	1	2	5	–	8
$\sum$	122	122	1553	92	218	2107

Patterns in both the relative abundances of geese and cormorants revealed from the San Francisco Peninsula collections are thus the same as those previously documented at Emeryville. These results were obtained despite the fact that the temporal scale required by using abundance data reported for sites as units is extremely coarse-grained and considerable overlap exists in the occupation ranges of nearly all of the sites in the sample. To provide further independent tests, we turn to an internal chronological analysis of the avifaunal materials derived from the Yerba Buena Shellmound.

3.2. The Yerba Buena Shellmound

The Yerba Buena Shellmound was a prehistoric habitation/ cemetery complex first discovered in 1988 beneath the basement foundations of 19th and 20th century buildings, razed for new construction in downtown San Francisco. The site was subjected to a relatively low degree of historic-period disturbance as it was deeply buried by shifting windblown sands prior to European settlement of the region. During its occupation by native peoples between about 2000 and 1000 B.P., the site was situated atop a stable sand dune, 400 m north of an
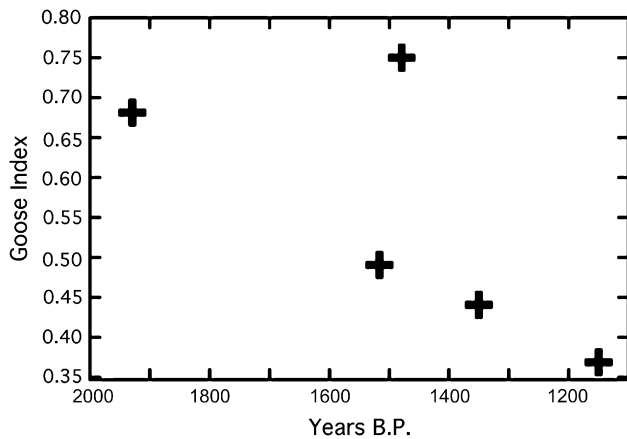

Fig. 2. The relationship between the goose index ($\sum$ NISP anserines/$\sum$ NISP anatids) and time for the San Francisco Peninsula assemblages.
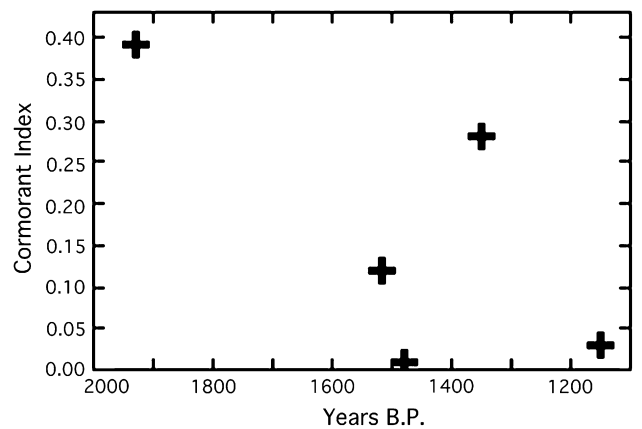

Fig. 3. The relationship between the cormorant index ($\sum$ NISP cormorants/ $\sum$ NISP birds) and time for the San Francisco Peninsula assemblages.

Fig. 4. Excavation of the Yerba Buena Shellmound showing stratigraphy and profile of Unit 178 at the southwestern edge of the site. (Photo credit: Archeo-Tec Consulting).

extensive brackish marsh and 800 m southwest of the San Francisco Bay shoreline [34].

The cultural sediments at the Yerba Buena site extended over a depth of roughly 1.3 m and were characterized by
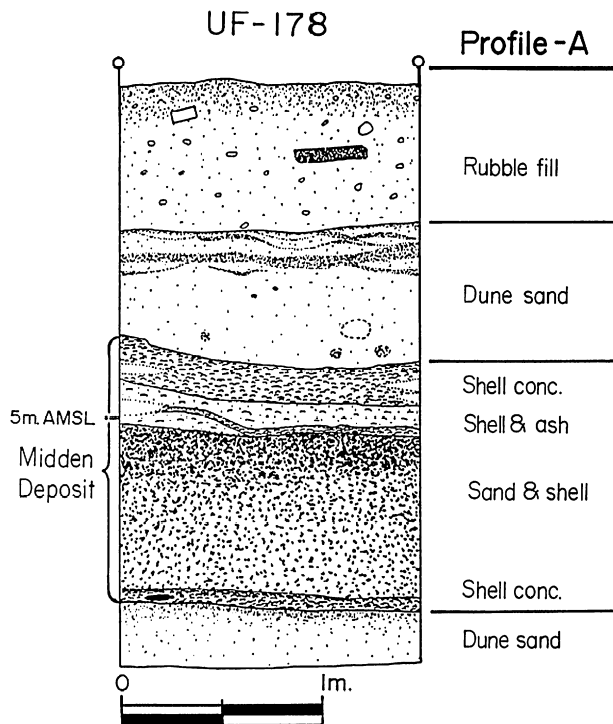

Fig. 5. Stratigraphic profile for Unit 178 of the Yerba Buena Shellmound. This site area was unusual in that the upper midden deposit contacted directly with natural dune sands that were capped with historic rubble fill. Throughout most of the site, however, the upper levels of the thick midden deposit were truncated by historic construction; sediments at this juncture consisted of a mix of historic rubble (e.g., bricks) and blocks of prehistoric midden. Much of the thick (3.5 m) historic overburden (rubble fill) was removed by heavy equipment prior to excavation. Level 1 (0–10 cm below surface) thus begins near the contact between the lower edge of the rubble fill (or dune sand, as in the case of UF-178) and the upper midden deposits [34].

a thick shell-rich midden deposit with occasional, discontinuous shell lenses and laminar ash and charcoal features (Figs. 4, 5). Few clearly defined stratigraphic markers extended for more than a couple meters within the main midden deposit, however, suggesting that bioturbation, aeolian mixing, and/or rapid deposition had affected the deposits. Indeed, extensive rodent krotovina in certain sections of the deposit attest to the presence of mixing. Still, shell valves often rested horizontally or normal to their depositional plane and many shell layers appeared intact with clear boundaries—indicating that a minimal degree of post-depositional disturbance characterized many other site areas. Given these features, and the lack of clearly definable strata within the main midden deposit at Yerba Buena, the site was excavated using arbitrary 10 cm levels and screened with 1/4- and 1/8-inch hardware cloth. In all, 76 units (area = 94 m^2 and volume = 76 m^3) were excavated using this strategy [34]. A north–south trending strip of the shellmound was not excavated allowing the division of faunal materials into East and West site areas.

Since sediment accretion at the site occurred over a ∼1000-year period with many centers of deposition, and post-depositional processes clearly disturbed parts of the original deposit, we cannot uncritically use depth below surface as an indicator of age for the Yerba Buena site. Fortunately, the distribution of 10 radiocarbon determinations from charcoal distributed across the Yerba Buena deposits allows us to evaluate the relationship between depth and age empirically (Table 3). These data, in addition to bracketing the site occupation between 1950 and 1010 ^{14}C yr B.P., show that depth below surface is positively correlated with ^{14}C years B.P. ($r = 0.61$, $P = 0.06$). This suggests that avifaunal data aggregated by 10-cm levels can be used as a chronological index to examine trends in bird hunting activities across the occupational history of the site.

We note too that previous analyses of the sites rich vertebrate fauna suggest that it provides a record of human foraging activities throughout the annual cycle. Temporal trends should thus be unaffected by seasonal migration schedules and other variables relating to the intra-annual availability of different avian taxa [7].

Since earlier work with the Yerba Buena avifauna did not provide identifications by depth for all of the recovered materials [7], we reanalyzed the collection, focusing initially

Table 3
Radiocarbon determinations from the Yerba Buena Shellmound (from [34])

Lab no.	Material	^{14}C yr B.P.	Level
Beta-42018	Charcoal	1010 ± 80	3
Beta-36300	Charcoal	1230 ± 80	1
Beta-42016	Charcoal	1400 ± 90	4
Beta-36298	Charcoal	1440 ± 90	8
Beta-36299	Carbon	1460 ± 70	3
Beta-38079	Charcoal	1510 ± 70	2
Beta-42017	Charcoal	1510 ± 70	9
Beta-36296	Charcoal	1610 ± 80	8
Beta-42019	Charcoal	1610 ± 80	3
Beta-36297	Charcoal	1950 ± 90	10

on the waterfowl and cormorant materials. However, only 20 cormorant specimens were recovered in the collection, thus precluding further analysis of them at the site. Finally, to provide two tests of the previously revealed patterns, we conducted separate analyses on the Yerba Buena waterfowl materials recovered from the East and West areas of the site (Appendix 1).

As with both the Emeryville and intersite San Francisco Peninsula analyses, highly significant declines through time in the abundances of geese are registered within the Yerba Buena deposits (Figs. 6 and 7) $\big($East : X^2_{trend} = 29.28, df = 1, P < 0.001; West : X^2_{trend} = 32.33, df = 1, P < 0.001$\big)$. Proportional declines in the abundances of the larger geese taxa (e.g., *Branta canadensis moffitti*, *Anser albifrons*, *Chen caerulescens*) compared to smaller geese (e.g., *Branta hutchinsii minima*, *Chen rossii*) are also apparent in these materials. In the West area assemblage that is represented by a much larger anserine sample size (N = 573), the trend is evident when all 14 levels are considered as separate analytical units $\big(X^2_{\mathrm{trend}}$ = 37.18, df = 1, P < 0.001$\big)$. This same approach failed to detect a decline in the smaller anserine collection (N = 335) from the East area $\big(X^2_{\mathrm{trend}}$ = 2.42, df = 1, P = 0.12$\big)$. However, when the relative frequencies of large and small geese from the upper levels (1–6) of the East area are aggregated as a unit, and compared to those from the conjoined lower level (7–12) samples, a significant decline in the abundance of large geese is evident in this site area as well $\big(X^2_{\mathrm{trend}}$ = 5.73, df = 1, P = 0.01$\big)$.

The same temporal patterns, consistent with anthropogenic depressions, have now been revealed internally within two sites on opposite sides of the San Francisco Bay—Emeryville and Yerba Buena—and among a set of five sites from the San Francisco Peninsula with different occupation dates. Again, previous analyses of paleoenvironmental data suggest that the trends are unrelated to climate-based environmental change [14]. We turn now to address what causal role, if any, intertaxonomic differences in bone density may have played in producing them.
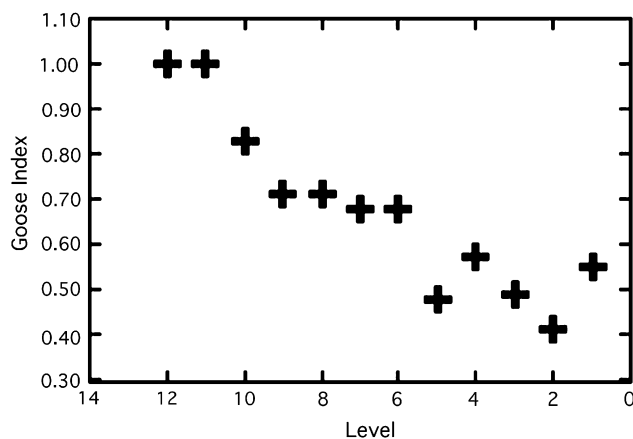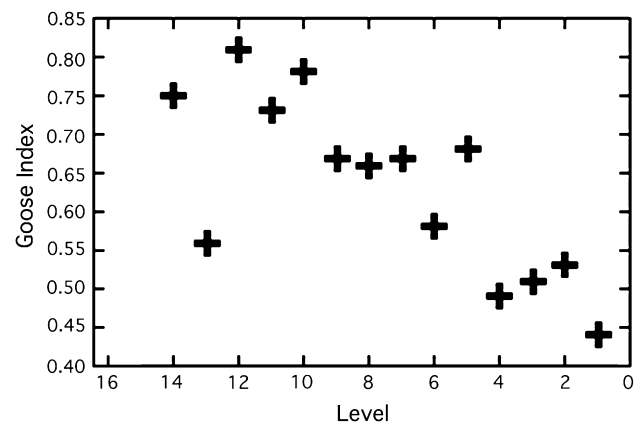

Fig. 7. The distribution of the goose index ($\sum$ NISP anserines/$\sum$ NISP anatids) by level (depth) for the West area of the Yerba Buena Shellmound.

4. Density-mediated attrition and avian taxonomic abundances

Density-mediated attrition is widely recognized as a critical taphonomic process affecting archaeological faunas [6,18,22, 41,43,44,48,49]. The focus of density analyses has been, however, on evaluating the effects of variation in the density of different bones within the skeletons of particular species (but see [43]). We present here new avian bone density values for a variety of bird taxa in order to evaluate whether the patterns we documented in taxonomic abundances could be explained by density-mediated attrition.

4.1. Skeletal element density values for cormorants, geese, and ducks

Complete skeletons of nine individual birds representing six different species were selected for bone density measurement. All of the selected species represent genera commonly found in North American archaeological avifaunas in general, and San Francisco Bay area assemblages in particular. The species measured include Double-crested Cormorant (*Phalacrocorax auritus*), Canada Goose (*Branta canadensis*), Gadwall (*Anas strepera*), Mallard (*Anas platyrhynchos*), Northern Pintail (*Anas acuta*), and Common Merganser (*Mergus merganser*). A mix of adult males and females and one juvenile bird were included in the sample given that archaeological avifaunas are typically comprised of such composites (see [24,25] for the issue of female medullary bone).

The full range of skeletal elements (exclusive of vertebrae, ribs, and phalanges) from each bird specimen were measured using a Norland XR-26 Dual Energy X-Ray Machine (DEXA), at the Department of Neonatology, Health Services Center, University of Utah. DEXA uses a dual photon absorptiometric system and measures bone mineral content (BMC) in grams. BMC of an element or element portion is then divided by a bone volume (V) estimate to produce "volume density" (gm/cm^3). As Cruz and Elkin [22] discuss, the Norland XR-26

Fig. 6. The distribution of the goose index ($\sum$ NISP anserines/$\sum$ NISP anatids) by level (depth) for the East area of the Yerba Buena Shellmound.

Table 4
Volume density (bone mineral content/volume) measurements by element for selected avian taxa

Element	Species (sex; catalog no.)								
	Phalacrocorax auritus (f; PSM 17186)	*P. auritus* (m; PSM 20106)	*Branta canadensis* (m; UMNH 33043)	*B. canadensis* (m; UMNH 40614)	*Anas strepera* (f; UMNH 22750)	*A. platyrhynchos* (m; UMNH 22710)	*A. acuta* (j; UMNH 22745)	*A. acuta* (f; UMNH 22760)	*Mergus merganser* (m; UMNH 22703)
Cranium	0.526	0.836	0.191	0.241	0.235	0.314	0.229	0.319	0.668
Dentary	0.872	0.803	0.324	0.627	0.196	0.322	0.253	0.899	0.536
Sternum	0.283	0.458	0.240	0.266	0.200	0.260	x	0.136	0.192
Furculum	0.243	0.613	0.516	0.462	0.370	0.404	x	0.201	0.574
Scapula	0.409	0.580	0.617	0.595	0.463	0.583	x	0.242	0.643
Coracoid	x	0.571	0.458	0.424	0.569	0.569	0.090	0.498	0.681
Humerus	0.588	0.596	0.403	0.551	0.477	0.484	0.563	0.454	0.618
Ulna	0.706	0.594	0.511	0.480	0.446	0.599	x	0.342	0.575
Radius	0.595	0.659	0.728	0.713	0.195	0.464	x	0.152	0.566
Carpometacarpus	0.628	0.565	0.548	0.571	0.573	0.758	x	0.372	0.560
Synsacrum	0.410	0.516	0.174	0.250	0.195	0.219	0.369	0.148	0.367
Femur	0.461	0.440	0.364	0.380	0.240	0.381	0.392	0.136	0.433
Tibiotarsus	0.453	0.532	0.576	0.515	0.455	0.503	0.141	0.331	0.607
Tarsometatarsus	0.532	0.521	0.433	0.395	0.252	0.241	0.433	0.124	0.478
Average BMC/V	0.516	0.592	0.434	0.462	0.348	0.436	0.309	0.311	0.536

PSM, Slater Musuem of Natural History; UMNH, Utah Museum of Natural History; j, juvenile; x, element not present or measurable.

DEXA provides BMC estimates for entire elements, rather than by linear scan sites. This feature is desirable in this context since bird element abundances are typically reported by element rather than by element portion, and it allows for an accurate estimate of bone volume using a water hydrostatic weighing method ([18]; see [44] for discussion on the advantages of this approach). The DEXA data were derived from single element scans, although mean values were used for paired elements. Our volume estimates, made with the water hydrostatic weighing method described in detail by Butler and Chatters [18], were derived from the mean values produced from three separate measurements made per element. The volume density values for the birds in our sample are provided by element in Table 4.

No significant differences exist in the average densities between individuals representing the same species in our sample (*P. auritus*: paired *t*-test = −1.90, df = 12, *P* > 0.05; *Branta canadensis*: paired *t*-test = −1.06, df = 13, *P* > 0.30; *Anas acuta*: paired *t*-test = −0.45, df = 7; *P* > 0.60). We obtained this result despite the fact that the two *P. auritus* specimens were from different sexes and juvenile and adult *A. acuta* specimens were measured.

Paired *t*-test comparisons of element densities between different species, however, showed many significant differences (Table 5). As has long been suggested by arguments based on functional anatomy [4,33,47], and water displacement-based density estimates on selected elements [35], the average skeletal densities for the two diving taxa—*P. auritus* and *Mergus merganser*—are no different from each other but are significantly higher than all of the other taxa in the sample. In addition, and of particular relevance here, the goose species in the sample—*B. canadensis*— displays a significantly higher average skeletal density than two of the ducks in the sample— *Anas strepera* and *A. acuta*. These data suggest that insofar as density is an important factor influencing avian bone survivorship in archaeological faunas, temporal trends in the relative taxonomic abundances of these taxa could be influenced by this variable.

4.2. Bone density and changing waterfowl abundances at Yerba Buena

As described above, significant declines through time in the abundance of geese compared to ducks were documented

Table 5
Matrix of paired *t*-test statistics for comparisons of average bone density between selected avian taxa

	P. auritus	*B. canadensis*	*A. strepera*	*A. platyrhynchos*	*A. acuta*
Phalacrocorax auritus	x	x	x	x	x
Branta canadensis	−2.401*	x	x	x	x
Anas strepera	−4.10***	−2.4*	x	x	x
Anas platyrhynchos	−2.46*	−0.38	4.08***	x	x
Anas acuta	−10.45***	−3.10**	−1.16	−2.86**	x
Mergus merganser	−0.59	2.32*	5.53***	2.74**	6.00***

*Significant at *P* < 0.05; **Significant at *P* < 0.01; ***Significant at *P* < 0.001.

across the occupational history of the Yerba Buena Shell-mound. If these declines resulted from density-mediated attrition, then temporal trends should be found in the extent of attrition observed in these faunas. More specifically, if ducks are proportionately underrepresented in the deeper, older sediments because they are characterized by lower density values and hence lower survivorship potential, then trends by depth in the volume density of the represented duck elements should be observed in the collection. We test this in several ways independently with the East and West area assemblages from Yerba Buena.

We use NISP values to measure element abundances here following Grayson and Frey [31]. However, to minimize the effects of fragmentation on these values, we attempted identifications only for relatively complete specimens (e.g., mostly whole proximal or distal ends of longbones; substantial cranium, sternum, and pelvis fragments) as described in [14].

In the first approach, we determine if significant correlations between duck skeletal element abundances and volume density exist in these deposits and, if so, do those correlations weaken through time, as the relative abundance of ducks increases. In the second approach, we evaluate the degree to which the average density of the represented duck elements increases with depth and correlates with their overall abundance relative to geese. In both analyses, the densities for the different duck elements were obtained by averaging the values presented for the four duck taxa in Table 4 (Table 6). This was required since the vast majority of duck identifications at Yerba Buena were made at the subfamily level (i.e., Anatinae), rather than at the tribe or genus level. There are, as we documented above, significant differences in element densities among some of the ducks in our sample (e.g., *Anas* vs. *Mergus*).

In both site areas at Yerba Buena, the element abundances for ducks are correlated with their densities: high-density elements are significantly more abundant than low-density
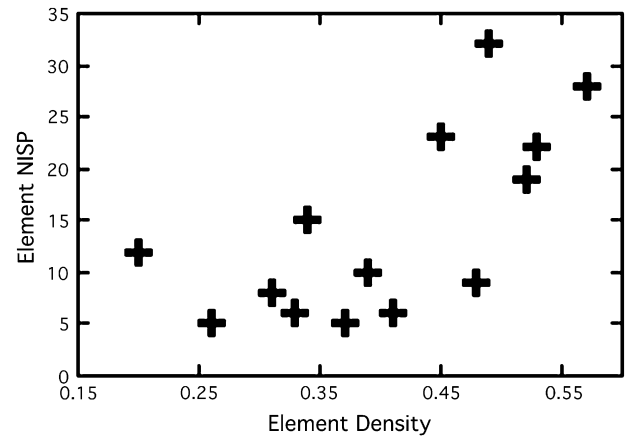

Fig. 8. The relationship between duck element abundances and density for the East area of the Yerba Buena Shellmound (all levels combined).

elements (Figs. 8 and 9; East: $r_s = 0.66$, $P = 0.01$; West: $r_s = 0.67$, $P = 0.01$). As has been repeatedly documented in mammalian faunas [49,44] and with limited work with fishes [18,19] and birds [22,35], density-mediated attrition appears to have structured duck element abundances at this site. But more significantly, no trends in attrition by depth, or through time, can be detected in these correlations (Figs. 10 and 11). In neither site area, are the Spearman's rho values between duck element abundances and density correlated with depth (East: $r_s = -0.50$, $P > 0.20$; West: $r_s = -0.23$, $P > 0.50$). And in only three individual 10 cm levels of the site (East: Level 4; West: Levels 1 and 8) were correlations, significant at .01, detected between duck element abundances and their densities. Moreover, when these three levels are removed from the analysis comparing the abundance of geese and ducks through time, there are still significant linear declines in geese for both site areas $\left(\text{East}: X^2_{trend} = 29.95, \text{df} = 10, P < 0.001; \text{West}: X^2_{trend} = 19.23, \text{df} = 11, P < 0.001\right)$.

Table 6
Average duck element volume densities (bone mineral content/volume)[a]

Element	Mean volume density
Cranium	0.37
Dentary	0.41
Sternum	0.20
Furculum	0.39
Scapula	0.48
Coracoid	0.53
Humerus	0.52
Ulna	0.49
Radius	0.34
Carpometacarpus	0.57
Synsacrum	0.26
Femur	0.33
Tibiotarsus	0.45
Tarsometatarsus	0.31

[a] Data derived from Table 4 (columns 6–10); a single value for *A. acuta* (mean of juvenile and adult) was used in these calculations.
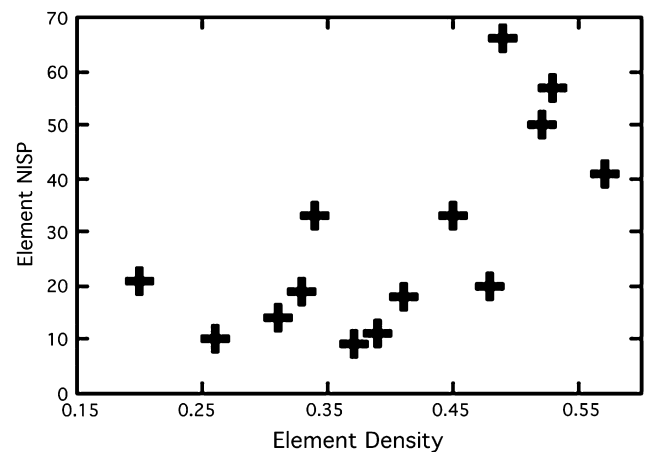

Fig. 9. The relationship between duck element abundances and density for the West area of the Yerba Buena Shellmound (all levels combined).
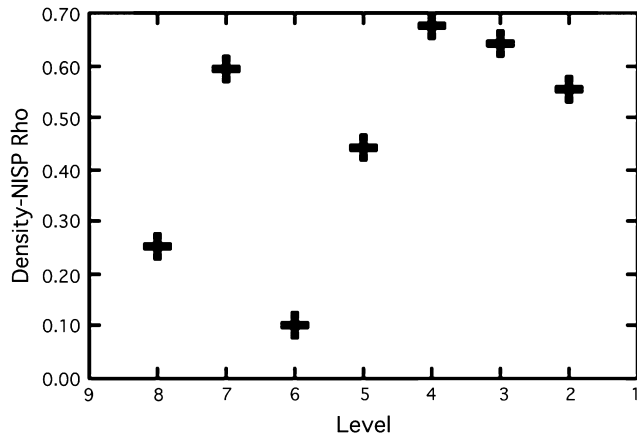
Fig. 10. Spearman's rho values between duck element abundances and density plotted by level (depth) for the East area of the Yerba Buena Shellmound.

Fig. 12. Mean density of the represented duck elements by level (depth) for the East area of the Yerba Buena Shellmound. (Only levels with duck NISP values > 10 were included in this analysis.)

To further explore the potential role of density-mediated attrition in these collections, we calculated the mean density of the duck elements represented per level for the two site areas using the formula: $\sum(NISP_i \times Density_i)/\sum NISP$, where the subscript "$i$" represents a particular skeletal element. As Figs. 12 and 13 show, virtually no changes through time are evident in the mean duck element density values for either the East or West site areas of Yerba Buena. Mean density is also not correlated with either depth or the goose index values for either of the site areas (East: mean density vs. depth, $r_s = 0.43$, $P = 0.26$; mean density vs. goose index, $r_s = -0.304$, $P = 0.42$; West: mean density vs. depth, $r_s = -0.14$, $P = 0.70$; mean density vs. goose index, $r_s = -0.258$, $P = 0.47$).

5. Bone density and the cormorant decline

Declining abundances of cormorant and goose remains from five sites on the San Francisco Peninsula duplicate the patterns previously documented in detail at the Emeryville

Shellmound. In addition, direct quantitative analyses of element abundances in relation to density with the waterfowl materials at Yerba Buena provide no suggestion that the trends in the relative abundances of those taxa are related to density-mediated attrition. And while we were unable to conduct analogous tests with the cormorant materials from Yerba Buena because they were so poorly represented at the site, more qualitative evaluations considering the high average density values they provided, suggest this variable is unlikely to have influenced their dramatic decline in San Francisco Bay area faunas after 1400 B.P.

As Table 5 shows, *Phalacrocorax auritus* produced significantly higher average skeletal density values than all but one of the species in the sample. Insofar as density influences bone survivorship, cormorants should be well represented, perhaps even over-represented compared to other taxa, in sediments where they were deposited. The pattern, however, is that cormorant bones are very abundant in the earlier deposits but they are virtually absent from the more recent ones. While it could be argued that they are over-represented in older strata because

Fig. 11. Spearman's rho values between duck element abundances and density plotted by level (depth) for the West area of the Yerba Buena Shellmound.
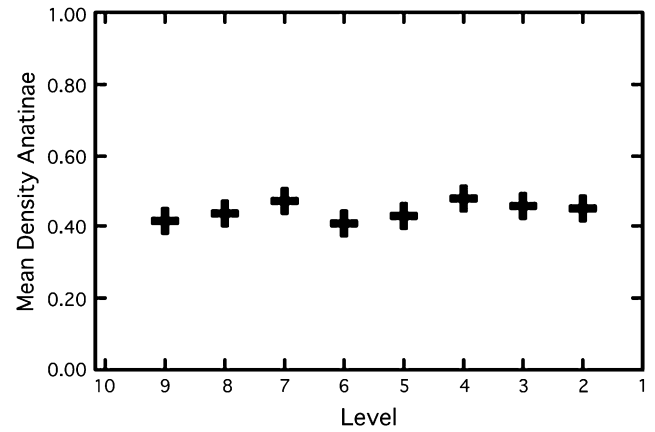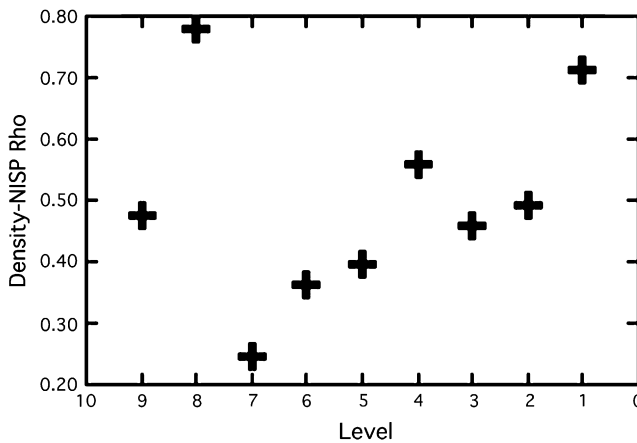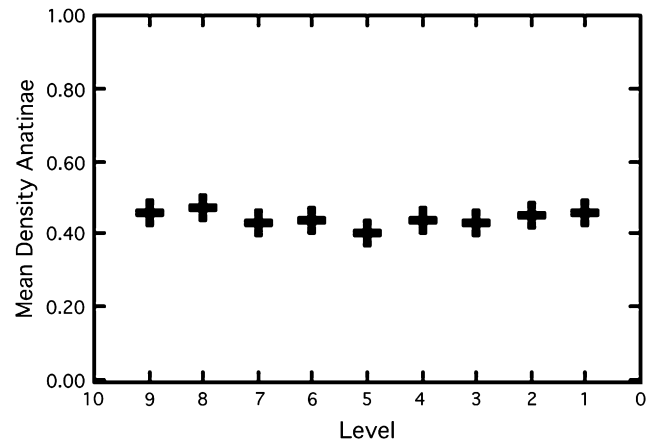

Fig. 13. Mean density of the represented duck elements by level (depth) for the West area of the Yerba Buena Shellmound. (Only levels with duck NISP values > 10 were included in this analysis.)
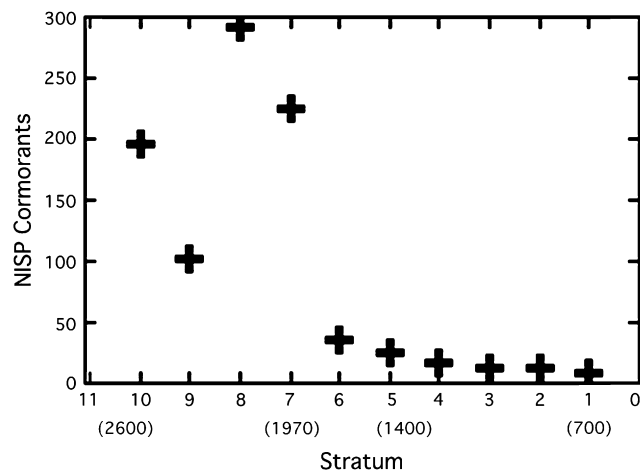
Fig. 14. Distribution of cormorant NISP values by stratum at the Emeryville Shellmound (data from [14]).

the bones from lower density taxa have disintegrated, even the absolute abundances of cormorant bones reveals that they vanish from Bay area avifaunas after about 1400 B.P. (Fig. 14). Moreover, the detailed data on cormorant age structure provided at Emeryville shows that the remains of cormorant chicks and juveniles—materials almost surely exhibiting lower densities than adult bones—are proportionately overrepresented, compared to adults, in the earlier deposits. Density-mediated attrition, thus, seems very unlikely to have played a role in producing the regional decline in late Holocene cormorant abundances.

6. Conclusion

Although numerous cases of prehistoric resource depression have been reported, only two involving continental bird populations have been documented in detail [5,14]. One of those, recently derived from analyses of the Emeryville Shellmound avifauna, suggested that expanding late Holocene human populations of the San Francisco Bay area caused significant declines in regional cormorant, waterfowl, and shorebird populations. While the trends were fully consistent with many other aspects of the vertebrate fauna [11,13,14], the results were derived from a single site located in the eastern part of the San Francisco Bay area and did not consider the potentially confounding effect of bone density on patterns in relative taxonomic abundances. We conducted an independent test of the avian resource depression hypothesis here by analyzing avifaunal remains from five additional sites located on the San Francisco Peninsula and assessing the role of density-mediated attrition.

Analysis of avifaunal materials from these sites showed significant declines through time in the relative abundance of both geese and cormorants between about 2000 and 700 B.P. Identical trends were documented by internal analyses of the avifauna from two separate areas of the Yerba Buena Shellmound—the site that produced the single largest avifaunal collection on the Peninsula. The potential effects of density-

mediated attrition on these trends were assessed by deriving volume density values from nine bird specimens, representing six species, including cormorants, geese, and ducks. These data were used in several different approaches to determine if variation in the densities of the represented avian skeletal elements was correlated with the trends in taxonomic abundances. Collectively, the data and analyses presented here suggest that while the effects of density-mediated attrition are readily detectable in the Yerba Buena waterfowl assemblage, there is no evidence that it varied systematically through time to produce the revealed patterns in taxonomic abundances. Resource depression thus remains a viable hypothesis for the declining abundances of geese in the region. More qualitative considerations regarding trends in cormorant abundances suggest bone density is unlikely to have played a key role in producing the regionally consistent temporal trend in cormorant abundances.

The avifaunal data presently available from the San Francisco Bay area strongly suggests that late Holocene hunters had substantial impacts on both waterfowl and cormorant populations in this setting, just as previous work has shown that they did for large-sized, economically attractive, species of molluscs, fishes, and mammals [9,10,11,13]. Resource depression has now been documented from a taxonomically comprehensive list of high-return animal prey types in this setting. This conclusion not only has implications for a diversity of issues relating to trends in human behavior during the late Holocene of California [16,39], but also is relevant to modern conservation biology and issues that require information on long-term population histories [14,27,28].

The data and methodologies developed here may also prove useful in evaluating trends in relative abundance data in other analyses of prehistoric resource depression. While the trends in avian relative abundances documented for the San Francisco Bay area sites do not appear to be related to density-mediated attrition, analogous trends in other contexts may show otherwise.

Finally, in addition to playing a role in the evaluation of trends in relative taxonomic abundances, the data on avian bone density provided here may help address a number of other issues relating to anatomical part representation. These include, but are not limited to, the symbolic use of birds, differential transport and processing, and the evaluation of the depositional origin of archaeological avifaunas [4,5,23,35,47].

Appendix 1

Table A1
Numbers of identified anserine elements by level for the East area of the Yerba Buena Shellmound[a]

Element	Level												$\sum$
	1	2	3	4	5	6	7	8	9	10	11	12	
Carpometacarpus			3	6	4	4	4	3	2	1	1	1	29
Coracoid	3	3	4	8	4	11	8	4	4	3	3	2	57
Cranium				1			1						2
Cuneiform				1									1
Femur	2		1	2	3	2	4	4	1		1		20
Furculum		1	1			1	2			2			7
Humerus		3	5	8	7	15	14	4	4	1	1	1	63
Mandible				1		2	1						4
Pelvis		2	1							1	1		5
Phalanx 1 (wing)				1	3	3	2	4	2				15
Phalanx 2 (wing)	1		1		1		1	1	2				7
Radius	1			2	2	3	1	1	1		1		12
Scapholunar							1						1
Scapula		2	2	1	3	4	6	3	2		1		24
Sternum	1	1		1			1	2		3	2	1	12
Synsacrum								1					1
Tarsometatarsus								1	1				2
Tibiotarsus		3		4	3	2	2	6	2	3	1		26
Ulna	2		1	2	11	9	3	4	4	1			37
Vertebra		1	1		1	2	1	4					10
$\sum$	10	16	20	38	42	58	52	42	25	15	12	5	335

  [a] The materials reported here (Appendix 1) and those described by Broughton [7] represent slightly different subsets of the Yerba Buena fauna. Broughton did not report on materials from the disturbed upper layers that contained historic-era fauna, but did describe specimens within the main midden that lacked depth (level) associations. Here, we report all anatid materials from the site that have secure level associations.

Table A2
Numbers of identified duck elements by level for the East area of the Yerba Buena Shellmound

Element	Level										$\sum$
	1	2	3	4	5	6	7	8	9	10	
Carpometacarpus	3	3	5	5	7		3		2		28
Coracoid	1	4	1	5	2	2	3	3	1		22
Cranium					1	1	1	1	1		5
Cuneiform						1					1
Femur				2		3		1			6
Furculum	2	2	1	1	3	1					10
Humerus		1	2	2	5	4	2	3			19
Mandible		1	2	1	1	1					6
Pelvis					1	2		1	1		5
Phalanx 1 (wing)					1	1					2
Phalanx 2 (wing)					1					1	2
Premaxilla					1					1	2
Radius		3	1	1	1	2	4	1	2		15
Scapula		1	3		2	2			1		9
Sternum	1	2	2		4	2			1		12
Tarsometatarsus					4	2		2			8
Tibiotarsus		1	1	4	5	2	7	3			23
Ulna	1	5	3	7	5	2	5	2	1	1	32
Vertebra						1					1
$\sum$	8	23	21	29	45	27	25	17	10	3	208

Table A3
Numbers of identified large anserines[a] by element and level for the East area of the Yerba Buena Shellmound

Element	1	2	3	4	5	6	7	8	9	10	11	12	Σ
Carpometacarpus	1					2		2	1	1	1		8
Coracoid	2	3	2	5		3	3	2	4	3		1	28
Cranium	1			1									2
Femur		1		2		1		1	1				6
Furculum	1			2	1	1							5
Humerus	3	1	1	2	2	8	9	3	1	1	1	1	33
Mandible					1								1
Pelvis			1	1		1		1					4
Phalanx 1 (wing)			1		2	2	1		2				8
Phalanx 2 (wing)				1	1	1	1	1					5
Radius			1	1	1	2	1	1	1				8
Scapholunar							1						1
Scapula	1	1		1		3	2	2					10
Sternum	1	1			1	2	3	1					9
Synsacrum						1		1					2
Tarsometatarsus										1			1
Tibiotarsus		3	2	2	1	2	3	2	1	1			17
Ulna	2	1	2	2	1	6	1	3	3	1			22
Vertebra		1		1		2	1	4	1				10
Σ	8	14	7	17	9	33	26	27	17	13	5	4	180

a The large anserine category includes elements identified as, or matching the size of, Chen caerulescens, Branta canadensis parvipes, B.c. moffitti, or Anser albifrons.

Table A4
Numbers of identified small anserines[a] by element and level for the East area of the Yerba Buena Shellmound

Element	1	2	3	4	5	6	7	8	9	10	11	12	Σ
Carpometacarpus			2	6	4	2	4	1	1		1		21
Coracoid		1	2	3	4	8	5	2			3	1	29
Cuneiform				1									1
Femur			1	1	3	1	3	3	1		1		14
Furculum			1		1								2
Humerus			4	5	5	7	5	1	3				30
Mandible				1		1	1						3
Pelvis						1							1
Phalanx 1 (wing)				1	3	1	1	1					7
Phalanx 2 (wing)					1	1							2
Radius				1	1	1			1				4
Scapula			1	2	2	1	4	1	2	1			14
Sternum					1		2						3
Tibiotarsus			1	2	1	2	1	1		1			9
Ulna	2	1	1	2	2	3	1	1	1		1		15
Σ	2	2	13	21	33	25	26	15	8	2	7	1	155

a The small anserine category includes elements identified as, or matching the size of, Branta hutchinsii minima, Chen rossi, or Branta bernicla.

Table A5
Numbers of identified anserine elements by level for the West area of the Yerba Buena Shellmound

Element	Level														Σ
	1	2	3	4	5	6	7	8	9	10	11	12	13	14	
Carpometacarpus	3	7	7	6	4	6	2	4	4	4	1	3		2	53
Coracoid	15	9	15	9	7	10	8	3	4	3	3	2			88
Cranium	1	1	1			1	1								5
Cuneiform		1		1											2
Femur	5	2	1	1	4	2	5	1					1		26
Foot phalanges	1	1	1	1											5
Furculum	2	4	1	2	2	5	4					1			13
Humerus	8	8	13	9	9	5	4	4	4	1					71
Mandible	2	2	1	1	3	3	1								13
Pelvis		3	5	3	3	2	5	4	2	2	1	1	1		17
Phalanx 1 (wing)	2	3	4	4	5	5	4	2	2	1	2	2	1		32
Phalanx 2 (wing)			2	1	2	2						1			15
Premaxilla			3	3											1
Radius	4	3	8	5	2	1	2	4	1	4		1	1	1	36
Scapula	6	9	4	4	2	6	4	2	1	2	1	2			44
Sternum	3	2	4	4			3	3	1	3	1	1			25
Synsacrum			2		1	1		1	1	1					1
Tarsometatarsus	2	4	3	2	1	2	5	7	5	3					17
Tibiotarsus	4	5	8	8	4	6	6	5	6	6					33
Ulna	5	5	1	1	2	3	3	4	1	1	1	1	1	1	61
Vertebra	1	1													15
Σ	61	77	78	52	52	50	54	48	26	35	19	13	5	3	573

Table A6
Numbers of duck elements by level for the West area of the Yerba Buena Shellmound

Element	Level														Σ
	1	2	3	4	5	6	7	8	9	10	11	12	13	14	
Carpometacarpus	6	10	5	9	2	2	3	3	1						41
Coracoid	8	5	10	3	5	8	7	4	4	4	3				57
Cranium	2	1	2	2			1	1							9
Cuneiform	1														1
Femur	1	2	4	3	3	3	2		1						19
Furculum	3	2	1	2	1	1	1					1			11
Humerus	9	13	7	6	3	2		1		3			1		50
Mandible	4	1	4	3	3	1	3		3				1		18
Pelvis	2	1	4	2	1	3	1				1				10
Phalanx 1 (wing)	3	2	2	2	1	2	1	1							7
Phalanx 2 (wing)	3	1	1		1		2	2	2	3			1		10
Radius	6	7	8	3	3	2	2	4	4	4	1	1			33
Scapula	2	2	3	4	3	1	2	2							20
Sternum		5	5	5	1	3	2								21
Synsacrum															1
Tarsometatarsus	3	3	1	1	1	1	1	1	1	1	1			1	14
Tibiotarsus	10	4	8	1	1	3	2	2	4	1	1	1	1	1	33
Ulna	17	11	10	7	1	6	4	4	4	1	1				66
Vertebra							2	2						1	6
Σ	78	68	76	54	25	36	27	25	13	10	7	3	4	1	427

Table A7

Numbers of identified large anserines[a] by element and level for the West area of the Yerba Buena Shellmound

Element	Level													Σ
	1	2	3	4	5	6	7	8	9	10	11	12	13	
Carpometacarpus	1	4	5	2	3	1	1	1	3		1	1	1	24
Coracoid	6	1	10	8	2	7	7	1	3	2	2	1	1	51
Cranium	1	1							1					4
Cuneiform	1													1
Femur	1			1		1	1	1						6
Foot phalanges	1				1				2					4
Furculum	1	2	1		1	2								7
Humerus	5	1	6	6	6	3	3	3	3	1	4			42
Mandible		2	1	1		1								5
Pelvis		3	3		2	1	1	1			1	1		13
Phalanx 1 (wing)	1	2	3	1	4	1	2	1	1	1	1	2		20
Phalanx 2 (wing)		1	1				1	1						5
Radius	1	2	2	1	2	2	1	2		2	1	1		15
Scapula	1	1	4	3	2	3	2	1	1	1	1	1		17
Sternum	1	2	4	3		1	2	4	1	2	1			13
Tarsometatarsus		2	1	2	2	1	2	1	3	3	2	1		10
Tibiotarsus	3	2	4	4	3	3	3	4	5	4	1	2	1	34
Ulna		2	1			2	3	2	5		1	1		15
Vertebra		1		1				2						15
Σ	23	27	40	32	27	26	28	30	20	18	16	9	3	299

[a] The large anserine category includes elements identified as, or matching the size of, *Chen caerulescens, Branta canadensis parvipes, B.c. moffitti,* or *Anser albifrons.*

Table A8

Numbers of identified small anserines[a] by element and level for the West area of the Yerba Buena Shellmound

Element	Level														Σ
	1	2	3	4	5	6	7	8	9	10	11	12	13	14	
Carpometacarpus	2	3	2	4	5	3	1	1	1	3		2			29
Coracoid	9	8	5	1	5	3	3	1	1		1	1		2	37
Cranium	1		1												1
Cuneiform															1
Femur	4	2	1	4	3	1	5	1	2						20
Foot phalanges		1	1												1
Furculum	1	2	1		2	1	1	1							6
Humerus	3	7	7	3	3	2	1	1	1			1			29
Mandible				1	3	2	3	1	1						8
Pelvis		2	2	1	1	1		1							4
Phalanx 1 (wing)	1	2	1	2	1	2	3	1	2	1					12
Phalanx 2 (wing)		1		2	2	2	1	2		1				1	10
Premaxilla															1
Radius	3	5	2	2	3	3	1	2	2	2					21
Scapula	6	8	7		3	1	2		1	1					27
Sternum	2	2		1	1	1	2	3							12
Synsacrum						1									1
Tarsometatarsus	1	2	1	1	1	1	3	1							7
Tibiotarsus	3	5	3	1	1	3	3	3	1		1		1		20
Ulna	2	3	4	4	3	4	3	3	2	2		1	1		27
Σ	38	50	38	20	25	24	26	18	6	17	3	4	2	3	274

[a] The small anserine category includes elements identified as, or matching the size of, *Branta hutchinsii minima, Chen rossi,* or *Branta bernicla.*

References

[1] S. Baker, Report on the Fort Mason Archaeological Test Excavations, Archaeological Consultants, San Francisco, 1978.

[2] F.E. Bayham, Factors influencing the Archaic pattern of animal utilization, Kiva 44 (1979) 219–235.

[3] F.E. Bayham, A diachronic analysis of prehistoric animal exploitation at Ventana Cave, PhD dissertation, Department of Anthropology, Arizona State University, Phoenix, 1982.

[4] K. Bovy, Differential avian skeletal part distribution: explaining the abundance of wings, Journal of Archaeological Science 29 (2002) 965–978.

[5] K. Bovy, Effects of human hunting, Climate change and tectonic events on the waterbirds along the pacific northwest coast during the Late Holocene, PhD dissertation, Department of Anthropology, University of Washington, Seattle, 2005.

[6] C.K. Brain, The contribution of Namib Desert Hottentots to an understanding of australopithecine bone accumulations, Scientific Papers of the Namib Desert Research Station 39 (1969) 13–22.

[7] J.M. Broughton, Vertebrate fauna, in: E.M. Hattori, A.G. Pastron (Eds.), Prehistory of the Yerba Buena Site, San Francisco, California, Archeotec Consulting, Oakland, 1991.

[8] J.M. Broughton, Late Holocene resource intensification in the Sacramento Valley, California: the vertebrate evidence, Journal of Archaeological Science 21 (1994) 501–514.

[9] J.M. Broughton, Declines in mammalian foraging efficiency during the late Holocene, San Francisco Bay, California, Journal of Anthropological Archaeology 13 (1994) 371–401.

[10] J.M. Broughton, Widening diet breadth, declining foraging efficiency, and prehistoric harvest pressure: ichthyofaunal evidence from the Emeryville Shellmound, California, Antiquity 71 (1997) 845–862.

[11] J.M. Broughton, Resource Depression and Intensification during the Late Holocene, San Francisco Bay: Evidence from the Emeryville Shellmound Vertebrate Fauna, University of California, Berkeley, 1999.

[12] J.M. Broughton, Pre-Columbian human impact on California vertebrates: evidence from old bones and implications for wilderness policy, in: C. Kay, R. Simmons (Eds.), Wilderness and Political Ecology: Aboriginal Influences and the Original State of Nature, University of Utah Press, Salt Lake City, 2002, pp. 44–71.

[13] J.M. Broughton, Prey spatial structure and behavior affect archaeological tests of optimal foraging models: examples from the Emeryville Shellmound vertebrate fauna, World Archaeology 34 (2002) 60–83.

[14] J.M. Broughton, Prehistoric Human Impacts on California Birds: Evidence from the Emeryville Shellmound Avifauna, Ornithological Monographs 56, American Ornithologists' Union, Washington D.C., 2004.

[15] J.M. Broughton, D.K. Grayson, Diet breadth, adaptive change, and the White Mountains faunas, Journal of Archaeological Science 20 (1993) 331–336.

[16] J.M. Broughton, J. O'Connell, On evolutionary ecology, selectionist archaeology, and behavioral archaeology, American Antiquity 64 (1999) 153–165.

[17] V.L. Butler, Resource depression on the Northwest Coast of North America, Antiquity 74 (2000) 649–661.

[18] V.L. Butler, J.C. Chatters, The role of bone density in structuring prehistoric salmon bone assemblages, Journal of Archaeological Science 21 (1994) 413–424.

[19] V.L. Butler, R.A. Schroeder, Do digestive processes leave diagnostic traces on fish bones? Journal of Archaeological Science 25 (1998) 957–971.

[20] M.D. Cannon, Large mammal relative abundance in Pithouse and Pueblo period archaeofaunas from southwestern New Mexico: resource depression among the Mimbres-Mogollon? Journal of Anthropological Archaeology 19 (2000) 317–347.

[21] M.D. Cannon, Archaeofaunal relative abundance, sample size, and statistical methods, Journal of Archaeological Science 28 (2001) 185–195.

[22] I. Cruz, D. Elkin, Structural bone density of the lesser rhea (*Pterocnemia pennata*) (Aves: Rheidae): taphonomic and archaeological implications, Journal of Archaeological Science 30 (2003) 37–44.

[23] S. deFrance, Pleistocene marine birds from southern Peru: distinguishing human capture from El Niño-induced windfall, Journal of Archaeological Science 32 (2005) 1131–1146.

[24] F.J. Dirrigl Jr., Bone mineral density of wild turkey (*Meleagris gallopavo*) skeletal elements and its effect on differential survivorship, Journal of Archaeological Science 28 (2001) 817–832.

[25] F.J. Dirrigl, G.P. Dalsky, S.E. Warner, Dual-energy X-ray absorptiometry of birds: an examination of excised skeletal specimens, Journal of Veterinary Medicine A 51 (2004) 313–319.

[26] W.N. Eschmeyer, J. Schonewald, Identification and Analysis of Fort Mason Osteological Remains, Archaeological Sites SFR-29, 30, 31, San Francisco Co., California, California Academy of Sciences, San Francisco, 1981.

[27] R. Frankham, J.D. Ballou, D.A. Briscoe, Introduction to Conservation Genetics, Cambridge University Press, Cambridge, 2002.

[28] T.C. Glenn, S. Wolfgang, M.J. Braun, Effects of a population bottleneck on Whooping Crane mitochondrial DNA variation, Conservation Biology 13 (1999) 1097–1107.

[29] D.K. Grayson, Alpine faunas from the White Mountains, California: adaptive change in the late prehistoric Great Basin, Journal of Archaeological Science 18 (1991) 483–506.

[30] D.K. Grayson, The archaeological record of human impacts on animal populations, Journal of World Prehistory 15 (2001) 1–68.

[31] D.K. Grayson, C.J. Frey, Measuring skeletal part representation in archaeological faunas, Journal of Taphonomy 2 (2004) 27–42.

[32] J.T. Hall, D.D. Simons, Appendix IV: CA-SFR-113 fauna—mammals and birds, in: A.G. Pastron, M.R. Walsh (Eds.), Archaeological Excavations at CA-SFR-113, the Market Street Shell Midden, San Francisco, California, Coyote Press Archives of California Prehistory 25, Salinas, 1988, pp. 71–77.

[33] J.G. Harrison, Skull pneumaticity: skull pneumaticity in wildfowl in relation to their mode of life, The Wildfowl Trust Annual Report 9 (1958) 193–196.

[34] E.M. Hattori, A.G. Pastron, Prehistory of the Yerba Buena Site, San Francisco, California, Archeo-tec Consulting, Oakland, 1991.

[35] J. Higgins, Tùnel: a case study of avian zooarchaeology and taphonomy, Journal of Archaeological Science 26 (1999) 1449–1457.

[36] W.R. Hildebrandt, T.L. Jones, Evolution of marine mammal hunting: a view from the California and Oregon coasts, Journal of Anthropological Archaeology 11 (1992) 360–401.

[37] W.R. Hildebrandt, T.L. Jones, Depletion of prehistoric pinniped populations along the California and Oregon coasts: were humans the cause? in: C. Kay, R. Simmons (Eds.), Wilderness and Political Ecology: Aboriginal Influences and the Original State of Nature University of Utah Press, Salt Lake City, 2002, pp. 72–110.

[38] J. Janetski, Fremont hunting and resource intensification in the eastern Great Basin, Journal of Archaeological Science 24 (1997) 1075–1088.

[39] T.L. Jones, M.L. Raab, The rediscovery of California prehistory, in: M.L. Raab, T.L. Jones (Eds.), Prehistoric California: Archaeology and the Myth of Paradise, University of Utah Press, Salt Lake City, 2004, pp. 1–9.

[40] M. Josselyn, The Ecology of the San Francisco Bay Tidal Marshes: A Community Profile, U.S. Fish and Wildlife Service, Division of Biological Services, Washington D.C., 1983.

[41] L.A. Kreutzer, Bison and deer bone mineral densities: comparisons and implications for the interpretation of archaeological faunas, Journal of Archaeological Science 19 (1993) 271–294.

[42] A.V. Küchler, Map of the Natural Vegetation of California, University of Kansas, Lawrence, 1977.

[43] Y.M. Lam, X. Chen, O.M. Pearson, Intertaxonomic variability in patterns of bone density and the differential representation of bovid, cervid, and equid elements in the archaeological record, American Antiquity 64 (1999) 343–362.

[44] Y.M. Lam, O.M. Pearson, Bone density studies and the interpretation of the faunal record, Evolutionary Anthropology 14 (2005) 99–108.

[45] P. Lieberson, Appendix 4: faunal analysis of CA-SFR-112, in: A.G. Pastron, M.R. Walsh (Eds.), Archaeological Excavations at CA-SFR-112, the Stevenson Street Shellmound, San Francisco, California,

Coyote Press Archives of California Prehistory 21, Salinas, 1988, pp. 117–129.

[46] K.G. Lightfoot, E.M. Luby, Late Holocene in the San Francisco Bay area: temporal trends in the use and abandonment of shell mounds in the East Bay, in: J.M. Erlandson, T.L. Jones (Eds.), Catalysts to Complexity: Late Holocene Societies of the California Coast, Perspectives in California Archaeology, vol. 6, Cotsen Institute of Archaeology, University of California, Los Angeles, 2002, pp. 263–281.

[47] S.D. Livingston, The taphonomic interpretation of avian skeletal part frequencies, Journal of Archaeological Science 16 (1989) 537–547.

[48] R.L. Lyman, Bone density and differential survivorship of fossil classes, Journal of Anthropological Archaeology 3 (1984) 259–299.

[49] R.L. Lyman, Vertebrate Taphonomy, Cambridge University Press, Cambridge, 1994.

[50] R.L. Lyman, Pinniped behavior, foraging theory, and the depression of metapopulations and nondepression of a local population on the southern Northwest Coast of North America, Journal of Archaeological Science 22 (2003) 376–388.

[51] R.L. Lyman, Paleozoology in the service of conservation biology, Evolutionary Anthropology 15 (2006) 11–19.

[52] M. McCrossin, Paleoecological inferences from a faunal analysis of CA-SFr-07, Journal of California and Great Basin Anthropology 4 (1981) 138–141.

[53] L.A. Nagaoka, Explaining subsistence change in southern New Zealand using foraging theory models, World Archaeology 34 (2002) 84–102.

[54] N.C. Nelson, Shellmounds of the San Francisco Bay region, University of California Publications in American Archaeology and Ethnology 7 (1909) 309–356.

[55] A.G. Pastron, M.R. Walsh, Archaeological Excavations at CA-SFR-112, the Stevenson Street Shellmound, San Francisco California, Coyote Press Archives of California Prehistory 21, Salinas, 1988.

[56] A.G. Pastron, M.R. Walsh, Archaeological Excavations at CA-SFR-113, the Market Street Shell Midden, San Francisco, California, Coyote Press Archives of California Prehistory 25, Salinas, 1988.

[57] J.F. Porcasi, T.L. Jones, M.L. Raab, Trans-Holocene marine mammal exploitation on San Clemente Island, California: a tragedy of the commons revisted, Journal of Anthropological Archaeology 19 (2000) 200–220.

[58] M.O. Rudo, The prehistory of San Francisco, M.A. thesis, Department of Anthropology, San Francisco State University, San Francisco, 1982.

[59] D.W. Stephens, J.R. Krebs, Foraging Theory, Princeton University Press, Princeton, 1986.

[60] M.C. Stiner, N.D. Munro, T.A. Surovell, The tortosie and the hare: small-game use, the broad-spectrum revolution, and Paleolithic demography, Current Anthropology 41 (2000) 39–73.

[61] A. Ugan, Does size matter? Body size, mass collecting, and their implications for understanding prehistoric foraging behavior, American Antiquity 70 (2005) 75–90.

[62] A. Ugan, Climate, bone density, and resource depression: what is driving variation in large and small game in Fremont archaeofaunas? Journal of Anthropological Archaeology 24 (2005) 227–251.

[63] D.S. Wilson, Deducing the energy available in the environment: an application of optimal foraging theory, Biotropica 8 (1976) 96–103.

[64] J.H. Zar, Biostatistical Analysis, Prentice Hall, Upper Saddle River, 1996.